

UC Riverside

UC Riverside Previously Published Works

Title

Triphenyl phosphate-induced pericardial edema in zebrafish embryos is reversible following depuration in clean water.

Permalink

<https://escholarship.org/uc/item/5tn771ng>

Authors

Wiegand, Jenna

Hoang, John

Avila-Barnard, Sarah

et al.

Publication Date

2023-10-01

DOI

10.1016/j.aquatox.2023.106699

Peer reviewed



Published in final edited form as:

Aquat Toxicol. 2023 October ; 263: 106699. doi:10.1016/j.aquatox.2023.106699.

Triphenyl phosphate-induced pericardial edema in zebrafish embryos is reversible following depuration in clean water

Jenna Wiegand^a, John Hoang^a, Sarah Avila-Barnard^a, Charvita Nemarugommula^a, Megan Ha^a, Sharon Zhang^b, Heather M. Stapleton^b, David C. Volz^{a,*}

^aDepartment of Environmental Sciences, University of California, Riverside, CA 92521, United States

^bDivision of Environmental Sciences and Policy, Duke University, Durham, NC 27708, United States

Abstract

Triphenyl phosphate (TPHP) – a widely used organophosphate-based flame retardant – blocks cardiac looping during zebrafish development in a concentration-dependent manner, a phenotype that is dependent on disruption of embryonic osmoregulation and pericardial edema formation. However, it's currently unclear whether (1) TPHP-induced effects on osmoregulation are driven by direct TPHP-induced injury to the embryonic epidermis and (2) whether TPHP-induced pericardial edema is reversible or irreversible following cessation of exposure. Therefore, the objectives of this study were to determine whether TPHP-induced pericardial edema is reversible and whether TPHP causes injury to the embryonic epidermis by quantifying the number of DAPI-positive epidermal cells and analyzing the morphology of the yolk sac epithelium using scanning electron microscopy. First, we found that exposure to 5 μ M TPHP from 24–72 h post-fertilization (hpf) did not increase prolactin – a hormone that regulates ions and water levels – in embryonic zebrafish, whereas high ionic strength exposure media was associated with elevated levels of prolactin. Second, we found that exposure to 5 μ M TPHP from 24–72 hpf did not decrease DAPI-positive epidermal cells within the embryonic epithelium, and that co-exposure with 2.14 μ M fenretinide – a synthetic retinoid that promotes epithelial wound repair – from 24–72 hpf did not mitigate the prevalence of TPHP-induced epidermal folds within the yolk sac epithelium when embryos were exposed within high ionic strength exposure media. Finally, we found that the pericardial area and body length of embryos exposed to 5 μ M TPHP from 24–72 hpf were similar

This is an open access article under the CC BY-NC-ND license (<http://creativecommons.org/licenses/by-nc-nd/4.0/>).

*Corresponding author. david.volz@ucr.edu (D.C. Volz).

Declaration of Competing Interest

The authors declare that they have no known competing financial interests or personal relationships that could have appeared to influence the work reported in this paper.

CRediT authorship contribution statement

Jenna Wiegand: Conceptualization, Methodology, Validation, Formal analysis, Investigation, Writing – original draft, Writing – review & editing, Visualization. **John Hoang:** Methodology, Investigation. **Sarah Avila-Barnard:** Methodology, Investigation. **Charvita Nemarugommula:** Methodology, Investigation. **Megan Ha:** Methodology, Investigation. **Sharon Zhang:** Methodology, Investigation. **Heather M. Stapleton:** Resources, Writing – review & editing, Supervision, Project administration. **David C. Volz:** Conceptualization, Resources, Writing – review & editing, Supervision, Project administration, Funding acquisition.

Supplementary materials

Supplementary material associated with this article can be found, in the online version, at doi:10.1016/j.aquatox.2023.106699.

to vehicle-treated embryos at 120 hpf following transfer to clean water and depuration of TPHP from 72–120 hpf. Overall, our findings suggest that (1) the ionic strength of exposure media may influence the baseline physiology of zebrafish embryos; (2) TPHP does not cause direct injury to the embryonic epidermis; and (3) TPHP-induced effects on pericardial area and body length are reversible 48 h after transferring embryos to clean water.

Keywords

Zebrafish; Pericardial edema Osmoregulation; Triphenyl phosphate; Epidermis

1. Introduction

Fish maintain ionic and osmotic homeostasis to ensure optimal cellular and physiological processes (Guh et al., 2015). Similar to humans, this process is achieved by utilizing transepithelial transport mechanisms (Guh et al., 2015). However, unlike humans, fish regulate ionic and osmotic gradients between an external aquatic environment and an internal biological system (Guh et al., 2015). Osmoregulation has evolved to quickly adapt to changes in the aquatic environment, which can vary in osmolarity and ionic composition (Guh et al., 2015). Adult fish perform many ionic and osmoregulatory mechanisms within the gills, which have a similar role as the human kidney (Evans, 2008; Hwang & Lee, 2007). Within the gills, ionocytes represent major, mitochondria-rich cells that are responsible for the transport of ions and are functionally analogous to mammalian renal tubular cells (Dymowska et al., 2012; Evans, 2011; Guh et al., 2015; Hwang et al., 2011).

After fertilization of zebrafish eggs, ionocytes begin to differentiate at approximately 24 h post-fertilization (hpf) and are localized along the embryonic epidermis to facilitate transport of essential ions from the surrounding water into the developing embryo (Hwang & Chou, 2013). As the fish continues to develop, ionocytes migrate to the developing gills and the number of epidermal ionocytes decreases. Following migration of all ionocytes to the gills, the number of ionocytes ceases to increase (Ayson et al., 1994; Hiroi et al., 1999). Gill-localized ionocytes provide adequate respiratory and osmoregulatory capacity in order to meet the organism's physiological demands (Rombough, 2007). When the epidermis is injured, the basal cell layer promotes active cell migration, while the superficial layer utilizes a purse-string contraction to seal off the wound (Gault et al., 2014). If epidermal cells are damaged, surrounding fluid can disrupt the ion gradients, leading to osmotic and electrical changes within the epidermis such as osmotic shock (Kennard & Theriot, 2020). Osmotic shock may serve as an early cue for epidermal injury, as osmotic shock causes cell swelling, tissue damage within the embryo, and the promotion of cellular migration toward the injury (Chen et al., 2019; Gault et al., 2014).

Prolactin is a freshwater-adapting hormone in zebrafish (Breves et al., 2014) that regulates ions and water levels in vertebrates (McCormick & Bradshaw, 2006). Interestingly, prolactin has varying functions in different vertebrates, ranging from (1) wound healing, seasonal hair growth, and milk production in mammals (Foitzik et al., 2009); (2) increasing open-channel density of sodium channels in adult frog skin (Takada & Kasai, 2003); and (3) altering skin

permeability of osmoregulatory surfaces (gills, skin, kidney, intestine, bladder) in teleost fish (Manzon, 2002). Prolactin regulates the amount of Na^+ , K^+ , and Cl^- in embryonic zebrafish (Shu et al., 2016). If prolactin levels are impacted due to chemical exposure, this has the potential to affect the regulation of Na^+ , K^+ , and Cl^- ion transport, which is essential for normal zebrafish development.

Prior studies in our lab have found that triphenyl phosphate (TPHP) – a widely used organophosphate-based flame retardant – blocks cardiac looping during zebrafish development in a concentration-dependent manner, a phenotype that is dependent on pericardial edema formation (Isales et al., 2015; McGee et al., 2013; Mitchell et al., 2018; Reddam et al., 2019; Yozzo et al., 2013). Moreover, D-Mannitol – an osmotic diuretic that increases the osmolarity of the surrounding solution (Papich, 2016) – and fenretinide – a synthetic retinoid that may promote epithelial wound repair (Szymanski et al., 2020) – are both able to block TPHP-induced pericardial edema (Mitchell et al., 2018, 2019; Reddam et al., 2019; Wiegand et al., 2022, 2023). D-Mannitol does not impact TPHP uptake in embryos, demonstrating that mitigation of TPHP-induced pericardial edema is not an artifact of decreased embryonic doses of TPHP in the presence of D-Mannitol (Wiegand et al., 2023). TPHP-induced pericardial edema is also associated with increased epidermal ionocyte and epidermal fold formation on the yolk sac epithelium, phenotypes that are rescued by co-exposing embryos to D-Mannitol (Wiegand et al., 2022, 2023). Finally, TPHP-induced pericardial edema does not occur in exposure solutions of low ionic strength (e.g., reverse osmosis water), with edema formation only occurring in exposure solutions with higher ionic strength (e.g., conditioned water from a recirculating system) (Wiegand et al., 2023). Overall, our studies to date collectively suggest that TPHP-induced pericardial edema within zebrafish embryos may be dependent on epidermal injury and disruption of osmoregulation across the epidermis. However, it's currently unclear whether TPHP-induced pericardial edema is reversible or irreversible within embryonic zebrafish.

Using zebrafish as a model, the primary objectives of this study were to (1) determine whether TPHP affects the abundance of prolactin; (2) identify whether TPHP induces epidermal injury; and (3) determine whether TPHP-induced pericardial edema is reversible or irreversible. To accomplish these objectives, we first relied on whole-mount immunohistochemistry and automated image analysis to quantify the abundance of prolactin within embryonic zebrafish under varying exposure conditions. Second, we quantified the abundance of embryonic epidermal cells by utilizing DAPI-based, *in situ* staining and automated image analysis. Third, we utilized scanning electron microscopy to determine whether fenretinide blocks TPHP-altered morphology and/or organization of the yolk sac epithelium. Finally, we exposed embryos to TPHP from 24–72 hpf and, after transferring embryos to clean system water from 72–120 hpf, determined whether the severity of TPHP-induced pericardial edema was associated with TPHP uptake and depuration.

2. Materials and methods

2.1. Animals

Using previously described procedures (Mitchell et al., 2018), wildtype adult (strain 5D) zebrafish were maintained and bred on a recirculating system according to an Institutional

Animal Care and Use Committee-approved animal use protocol (#20210027) at the University of California, Riverside.

2.2. Chemicals

TPHP (99.5 % purity), D-mannitol (>98 % purity), and fenretinide (>99.3 % purity) were purchased from ChemService, Inc. (West Chester, PA, USA), Bio-Techne Corp. (Minneapolis, MN, USA), and Tocris Bioscience (Bristol, UK), respectively. Stock solutions of TPHP and fenretinide were prepared in liquid chromatography-grade dimethyl sulfoxide (DMSO) using previously described procedures (Wiegand et al., 2023). Working solutions of TPHP, fenretinide, and D-mannitol were prepared in particulate-free water using previously described procedures (Wiegand et al., 2023).

2.3. TPHP exposures

Immediately after spawning, fertilized eggs were collected and incubated using previously described procedures (Wiegand et al., 2023). Working solutions of vehicle (0.1 % DMSO), 250 mM D-mannitol, 2.14 μ M fenretinide, 5 μ M TPHP, 250 mM D-Mannitol + 5 μ M TPHP, or 2.14 μ M fenretinide + 5 μ M TPHP were prepared as described above. The concentrations of D-mannitol, fenretinide, and TPHP were selected based on our previously published studies (Mitchell et al., 2019; Reddam et al., 2019; Wiegand et al., 2022, 2023). Embryos (30 initial embryos per dish; three replicate dishes per treatment) were exposed under static conditions to each treatment solution from 24 to 72 hpf using previously described procedures (Wiegand et al., 2023). At 72 hpf, embryos were pooled into 1.5 mL microcentrifuge tubes according to each treatment replicate, fixed in 4 % paraformaldehyde (PFA) in 1X phosphate-buffered saline (PBS) overnight at 4°C, transferred to 1X PBS, and stored at 4°C for no longer than one month until imaging.

To determine whether TPHP-induced pericardial edema was reversible, working solutions of vehicle (0.1 % DMSO) and 5 μ M TPHP were prepared as described above. Embryos (30 initial embryos per dish; 12 replicate dishes per treatment) were exposed to vehicle (0.1 % DMSO) or 5 μ M TPHP from 24 to 72 hpf using previously described procedures (Wiegand et al., 2023). At 48 and 72 hpf, vehicle- and TPHP-treated embryos were collected from three replicate dishes per time-point and then fixed and stored as described above. Embryos within the remaining replicate dishes were transferred from vehicle or TPHP solutions into clean water from our recirculating water system and then incubated under a 14 h:10 h light-dark cycle at 28°C until 96 or 120 hpf. At 96 and 120 hpf, vehicle- and TPHP-treated embryos were collected from three replicate dishes per time-point and then fixed and stored as described above. Fixed embryos (coded by treatment group and replicate) were then transferred to black 384-well microplates containing 0.17 mm glass-bottom wells (Matrical Bioscience, Spokane, WA, USA), centrifuged at 140 rpm for 5 min, and imaged under transmitted light on our ImageXpress Micro XLS Widefield High-Content Screening System within MetaXpress 6.0.3.1658 (Molecular Devices, Sunnyvale, CA, USA). Body length, pericardial area, and yolk sac area were manually quantified within MetaXpress using images captured under transmitted light.

2.4. Whole-mount immunohistochemistry and automated imaging

Similar to previously described protocols (Yozzo et al., 2013), fixed embryos were labeled with 1:500 dilution of a prolactin-specific monoclonal antibody (INN-hPRL-1) (Life Technologies, Carlsbad, CA, USA) and 1:500 dilution of AlexaFluor 488-conjugated goat anti-mouse IgG₁ cross-adsorbed antibody (Thermo Fisher Scientific, Waltham, MA, USA) to quantify the abundance of prolactin. Labeled embryos were then imaged under transmitted light and a FITC filter as described above. Body length, pericardial area, and yolk sac area were manually quantified as described above, whereas prolactin was automatically quantified within MetaXpress using images captured under a FITC filter.

2.5. Quantification of the abundance of embryonic epidermal cells

Vehicle- and TPHP-treated embryos were stained with DAPI to quantify the abundance of cells within the embryonic epidermis. Following exposure from 24–72 hpf, 72-hpf embryos were fixed and stored as described above. Fixed embryos were then incubated at room temperature for 15 min in a DAPI-containing Fluoromount-G mounting medium (Thermo Fisher Scientific, Waltham, MA, USA) that was diluted 1:4 in 1X PBS. The solution was then aspirated, and embryos were washed with reverse osmosis (RO) water for 5 min while shaking. Embryos were then imaged under transmitted light and a DAPI filter as described above. The total area and number of DAPI-labeled epidermal cells were automatically quantified with a custom module within MetaXpress using images captured under a DAPI filter.

2.6. Quantification of embryonic doses of TPHP and DPHP

Embryonic doses of TPHP and diphenyl phosphate (DPHP, the primary metabolite of TPHP) were quantified at 48 hpf, 72 hpf, 96 hpf, and 120 hpf following exposure to vehicle (0.1 % DMSO) or 5 μ M TPHP from 24–72 hpf and following transfer to clean water from 72–120 hpf as described above. For each replicate (four replicate dishes per treatment per timepoint), analytes were extracted and quantified from ~30 embryos according to previously published methods (Mitchell et al., 2018). The method detection limits (MDLs) for TPHP and DPHP were 0.05 ng and 0.45 ng, respectively.

2.7. Scanning electron microscopy

Prior to imaging, embryos were exposed from 24–72 hpf within RO water, system water, or 2X embryo media (EM) (Wiegand et al., 2023) containing 0.1 % DMSO, 5 μ M TPHP, 2.14 μ M fenretinide, or 5 μ M TPHP + 2.14 μ M fenretinide as described above. At 72 hpf, all embryos were fixed and stored as described above. Fixed embryos were processed and imaged using a Hitachi Tabletop TM4000Plus Scanning Electron Microscope (SEM) according to previously described protocols (Wiegand et al., 2023).

2.8. Statistics

All data were analyzed within SPSS Statistics 24 using a general linear model (GLM) analysis of variance (ANOVA) ($\alpha = 0.05$) and Tukey-based multiple comparisons. Unlike a non-GLM-based ANOVA, a GLM ANOVA does not require normally distributed data nor equal sample sizes and variances across all treatment groups. Therefore, raw data can be

analyzed within a GLM ANOVA without the need for data transformations (e.g., log-based transformations) that artificially reduce variance and increase the probability of false positive hits (i.e., Type I errors). As individual embryos from each experiment were coded by treatment and replicate, we accounted for treatment-related effects as a Fixed Factor and replicate-to-replicate variability as a Random Factor within each GLM ANOVA.

3. Results

3.1. Ionic strength of exposure media is associated with elevated levels of prolactin

Relative to embryos exposed to vehicle (0.1 % DMSO) from 24–72 hpf, exposure to 5 μ M TPHP alone from 24–72 hpf across all three exposure media types (RO Water, System Water, or 2X EM) did not result in a significant increase in prolactin abundance (Fig. 1; Fig. S1). However, there was an upward trend in prolactin abundance as the ionic strength of exposure media increased from RO Water to System Water to 2X EM, while D-Mannitol alone and TPHP + D-Mannitol co-exposures suppressed prolactin levels across all exposure media types. Pericardial area, yolk sac area, and body length across all treatments were consistent with our prior studies (Isales et al., 2015; McGee et al., 2013; Mitchell et al., 2018; Reddam et al., 2019; Wiegand et al., 2022, 2023), where yolk sac area was not affected across treatments nor embryo media types and TPHP induced pericardial edema within embryos exposed within System Water and 2X EM (Fig. 1; Fig. S1).

3.2. TPHP does not decrease DAPI-positive cells within the embryonic epidermis

To determine if TPHP has the potential to decrease the number of epidermal cells, embryos were fixed and stained with DAPI following exposure to vehicle (0.1 % DMSO), 2.14 μ M Fenretinide, 250 mM D-Mannitol, 5 μ M TPHP, 5 μ M TPHP + 2.14 μ M Fenretinide, or 5 μ M TPHP + 250 mM D-Mannitol from 24–72 hpf. Embryos were then analyzed utilizing a custom module within MetaXpress to quantify individual cell nuclei and the total area of all nuclei present within the embryonic epidermis. These data were then divided by body length to normalize against embryo size. In RO Water and 2X EM, there were no significant differences in length-normalized total area of nuclei across all treatments. However, when exposed in System Water, 2.14 μ M Fenretinide, 5 μ M TPHP + 2.14 μ M Fenretinide, and 5 μ M TPHP + 250 mM D-Mannitol resulted in an increase in length-normalized total area of nuclei (Fig. 2; Fig. S2). Interestingly, there was only one treatment – 250 mM D-Mannitol in RO water – that resulted in a significant increase in length-normalized total cell count (Fig. 2; Fig. S2), although this effect was not observed within System Water nor 2X EM. Body length data were consistent with our prior studies (Isales et al., 2015; McGee et al., 2013; Mitchell et al., 2018, 2019; Reddam et al., 2019; Wiegand et al., 2022, 2023), where exposure to 5 μ M TPHP within System Water and 2X EM resulted in decreased body length relative to vehicle controls. However, co-exposure with 2.14 μ M Fenretinide or 250 mM D-Mannitol failed to mitigate TPHP-induced effects on body length (Fig. 2).

3.3. Fenretinide does not mitigate the prevalence of TPHP-induced epidermal folds

Within all SEM imaging locations and exposure media types, 5 μ M TPHP induced an increase in the prevalence of epidermal folds on the yolk sac epithelium relative to vehicle controls, with significant differences appearing in (1) Locations A and B in all three

exposure types, (2) Location C in System Water and 2X EM, and (3) Locations D and E in 2X EM (Fig. 3). Interestingly, contrary to our previous findings with D-Mannitol (Wiegand et al., 2023), fenretinide did not mitigate the prevalence of TPHP-induced epidermal folds when embryos were exposed within high ionic strength exposure media (Fig. 3). Finally, consistent with our prior studies (Wiegand et al., 2023), there was an elevation in the abundance of epidermal folds as a function of increasing ionic strength of exposure media from RO Water to System Water to 2X EM.

3.4. TPHP-induced effects on pericardial area and body length are reversible

To determine if embryos depurated TPHP after rapid uptake from 24–72 hpf, embryonic doses of TPHP and DPHP were quantified at 48 hpf, 72 hpf, 96 hpf, and 120 hpf. Embryonic doses of TPHP and DPHP were significantly decreased at 96 hpf and 120 hpf after embryos were transferred to clean System Water at 72 hpf (Fig. 4). Likewise, the severity of TPHP-induced effects on pericardial area and body length was decreased following transfer to clean System Water at 72 hpf, returning to levels similar to vehicle controls by 120 hpf (Fig. 5).

4. Discussion

Based on prior studies in embryonic zebrafish, we previously found that TPHP disrupted cardiac looping, induced pericardial edema and liver enlargement, increased ionocyte abundance, and decreased body length (Isales et al., 2015; McGee et al., 2013; Mitchell et al., 2018; Reddam et al., 2019; Wiegand et al., 2022, 2023). In our most recent study, we also found that TPHP-induced pericardial edema was dependent on the ionic strength of exposure media (Wiegand et al., 2023). Although ion-deficient conditions increase prolactin receptor a (*prlra*) in adult zebrafish (Breves et al., 2013), we found that the levels of prolactin in embryonic zebrafish were impacted by the ionic strength of exposure media and not TPHP exposure. Interestingly, prolactin is essential for zebrafish larvae to survive in freshwater, as it allows larval fish to adapt to varying ion levels in the surrounding water (Shu et al., 2016). Moreover, prolactin is a freshwater adaptation hormone (Breves et al., 2014; Manzon, 2002) that is necessary for regulation of the expression of specific ionocytes in zebrafish gills and skin throughout development (Breves et al., 2013, 2014). Therefore, our data suggest that an increase in prolactin as a function of increasing ionic strength of exposure media may be a compensatory response to maintain homeostasis within embryonic zebrafish.

Despite TPHP-induced effects on the yolk sac epithelium (Fig. 3; Wiegand et al., 2022), TPHP did not decrease DAPI-positive cells within the embryonic epidermis. Prior studies that have investigated embryonic zebrafish skin damage focus on the skin healing process, utilizing methods such as the tail wounding assay, immunohistochemistry, and transgenic lines (LeBert & Huttenlocher, 2014; Richardson, 2018; Rosowski, 2020). Only one study has utilized a neutral red dye to stain chemically-induced cell injury on the epidermis (Peng et al., 2018). DAPI-stained embryos revealed that TPHP did not decrease the total number of cell nuclei within the epidermis. Although DAPI can be used as a vital dye to identify live vs. dead cells, DAPI does not reveal non-lethal damage or if junctions between the

epidermal cells are being impacted by TPHP. Therefore, it is possible that, in the absence of epidermal cell death, TPHP may induce osmotic shock within the embryonic epidermis due to skin or junction damage, as osmotic shock may alter the ability of embryos to properly regulate ion uptake. Our past study found that the number of ionocytes increased following exposure to TPHP (Wiegand et al., 2022), a compensatory response that may have occurred as a result of regulating an increase in ion concentrations within the embryo.

Based on our most recent study, TPHP exposure resulted in an increase in epidermal folds on the yolk sac epithelium in embryonic zebrafish, and D-Mannitol (an osmoprotectant) was found to block this increase in epidermal folds (Wiegand et al., 2023). Fenretinide – a synthetic retinoid and pan-retinoic acid receptor agonist – was also previously found to reverse pericardial edema within TPHP-exposed embryos (Mitchell et al., 2018). Therefore, similar to D-Mannitol, we hypothesized that fenretinide may block a TPHP-induced increase in epidermal folds on the yolk sac epithelium. Contrary to our hypothesis, fenretinide did not block an increase in TPHP-induced epidermal folds, suggesting that fenretinide-mediated mitigation of TPHP-induced pericardial edema is independent – and possibly downstream – of TPHP-induced epidermal fold formation within the yolk sac epithelium. Interestingly, our findings also suggest that TPHP does not adversely impact the rate of yolk sac absorption during exposure (since yolk sac area was unaffected), and that the formation of TPHP-induced epidermal folds are independent of yolk sac absorption. Although little is known about how contaminants induce the formation of epidermal folds within embryonic zebrafish, it is possible that, given the role of the yolk sac epithelium in osmoregulation, chemically-induced alterations in epidermal folds may impact normal osmoregulation within the embryo (Breves et al., 2014; Dymowska et al., 2012; Evans, 2008, 2011; Gilmour, 2012; Hiroi & McCormick, 2012; Hwang & Lee, 2007; Hwang et al., 2011; Kumai & Perry, 2012; Wright & Wood, 2012).

Our prior studies also showed that TPHP-induced pericardial edema occurs when embryos are exposed to 5 μ M TPHP from 24–72 hpf (Isales et al., 2015; McGee et al., 2013; Mitchell et al., 2018; Reddam et al., 2019; Wiegand et al., 2022, 2023). To determine if TPHP-induced pericardial edema and decreased body length are reversible phenotypes during embryonic development, TPHP-exposed embryos were placed in clean (TPHP-free) system water from 72–120 hpf after being exposed to TPHP from 24–72 hpf. Interestingly, we found that, following transfer to clean water, TPHP-induced pericardial edema and body length were significantly mitigated by 96 hpf and 120 hpf in a time-dependent manner – a finding that was strongly associated with time-dependent depuration from 72–120 hpf. Moreover, there was an approximately 24 h lag between TPHP depuration vs. recovery of embryo morphology based on pericardial area and body length as endpoints, suggesting that TPHP-induced developmental toxicity may be reversible. Finally, the yolk sac area within TPHP-exposed embryos was not different from vehicle-treated embryos at 72, 96, and 120 hpf following depuration from 72–120 hpf, suggesting that (1) TPHP does not adversely impact the rate of yolk sac absorption during depuration and (2) the recovery of TPHP-induced effects on both length are independent of yolk sac absorption.

5. Conclusions

To our knowledge, this is the first study to investigate the role of epidermal injury and uptake/depuration kinetics in TPHP-induced pericardial edema within zebrafish embryos. First, we found that exposure to TPHP from 24–72 h post-fertilization (hp) did not increase prolactin in embryonic zebrafish, whereas high ionic strength exposure media was associated with elevated levels of prolactin. Second, we found that TPHP did not decrease DAPI-positive epidermal cells within the embryonic epithelium, and that fenretinide did not mitigate the prevalence of TPHP-induced epidermal folds within the yolk sac epithelium when embryos were exposed within high ionic strength exposure media. Finally, we found that the pericardial area and body length of TPHP-exposed embryos were comparable to vehicle-treated embryos following transfer to clean water and depuration of TPHP. Overall, our findings suggest that (1) the ionic strength of exposure media may influence the baseline physiology of zebrafish embryos; (2) TPHP does not cause direct injury to the embryonic epidermis; and (3) TPHP-induced effects on pericardial area and body length are reversible 48 h after transferring embryos to clean water.

Supplementary Material

Refer to Web version on PubMed Central for supplementary material.

Funding

Fellowship support was provided by the NRSA T32 Training Program [T32ES018827] to SAB. Research support was provided by a National Institutes of Health grant (R01ES027576) and USDA National Institute of Food and Agriculture Hatch Project (1009609) to DCV.

Data availability

Data will be made available on request.

References

- Ayson FG, Kaneko T, Hasegawa S, Hirano T, 1994. Development of mitochondrion-rich cells in the yolk-sac membrane of embryos and larvae of tilapia, *Oreochromis mossambicus*, in fresh water and seawater. *J. Exp. Zool.* 270 (2), 129–135. 10.1002/JEZ.1402700202.
- Breves JP, McCormick SD, Karlstrom RO, 2014. Prolactin and teleost ionocytes: new insights into cellular and molecular targets of prolactin in vertebrate epithelia. *Gen. Comp. Endocrinol.* 0, 21. 10.1016/J.YGCEN.2013.12.014.
- Breves JP, Serizier SB, Goffin V, McCormick SD, Karlstrom RO, 2013. Prolactin regulates transcription of the ion uptake Na⁺/Cl⁻ cotransporter (ncc) gene in zebrafish gill. *Mol. Cell. Endocrinol.* 369 (1–2), 98–106. 10.1016/j.mce.2013.01.021. [PubMed: 23395804]
- Chen T, Zhao H, Gao L, Song L, Yang F, Du J, 2019. Hypotonicity promotes epithelial gap closure by lamellipodial protrusion. *Prog. Biophys. Mol. Biol.* 148, 60–64. 10.1016/j.pbiomolbio.2017.09.021. [PubMed: 28962936]
- Dymowska AK, Hwang PP, Goss GG, 2012. Structure and function of ionocytes in the freshwater fish gill. *Respir. Physiol. Neurobiol.* 184 (3), 282–292. 10.1016/J.RESP.2012.08.025.
- Evans D, 2008. Teleost fish osmoregulation: what have we learned since august Krogh, homer smith, and ancel keys. *Am. J. Physiol. Regul. Integr. Comp. Physiol.* 295 (2) 10.1152/AJPREGU.90337.2008/SUPPL_FILE/DESCRIPTIONS.DOCX.

- Evans D, 2011. Freshwater fish gill ion transport: august Krogh to morpholinos and microprobes. *Acta Physiol.* 202 (3), 349–359. 10.1111/J.1748-1716.2010.02186.X.
- Foitzik K, Langan EA, Paus R, 2009. Prolactin and the skin: a dermatological perspective on an ancient pleiotropic peptide hormone. *J. Invest. Dermatol.* 129 (5), 1071–1087. 10.1038/JID.2008.348. [PubMed: 19110541]
- Gault WJ, Enyedi B, Niethammer P, 2014. Osmotic surveillance mediates rapid wound closure through nucleotide release. *J. Cell Biol.* 207 (6), 767–782. 10.1083/jcb.201408049. [PubMed: 25533845]
- Gilmour KM, 2012. New insights into the many functions of carbonic anhydrase in fish gills. *Respir. Physiol. Neurobiol.* 184 (3), 223–230. 10.1016/J.RESP.2012.06.001. [PubMed: 22706265]
- Guh YJ, Lin CH, Hwang PP, 2015. Osmoregulation in zebrafish: Ion transport mechanisms and functional regulation. *EXCLI J.* 14, 627–659. 10.17179/excli2015-246. [PubMed: 26600749]
- Hiroi J, Kaneko T, Tanaka M, 1999. In vivo sequential changes in chloride cell morphology in the yolk-sac membrane of mozambique tilapia (*Oreochromis mossambicus*) embryos and larvae during seawater adaptation. *J. Exp. Biol.* 24 (24), 3485–3495. 10.1242/JEB.202.24.3485, 202 Pt.
- Hiroi J, McCormick SD, 2012. New insights into gill ionocyte and ion transporter function in euryhaline and diadromous fish. *Respir. Physiol. Neurobiol.* 184 (3), 257–268. 10.1016/J.RESP.2012.07.019. [PubMed: 22850177]
- Hwang P, Lee TH, 2007. New insights into fish ion regulation and mitochondrion-rich cells. In: *Comparative Biochemistry and Physiology - A Molecular and Integrative Physiology*, 148. Pergamon, pp. 479–497. 10.1016/j.cbpa.2007.06.416. [PubMed: 17689996]
- Hwang P, Chou MY, 2013. Zebrafish as an animal model to study ion homeostasis. *Pflug. Arch.* 465 (9), 1233–1247. 10.1007/S00424-013-1269-1. *Eur. J. Physiol.*
- Hwang P, Lee TH, Lin LY, 2011. Ion regulation in fish gills: Recent progress in the cellular and molecular mechanisms. *Am. J. Physiol. Regul. Integr. Comp. Physiol.* 301 (1), 28–47. 10.1152/AJPREGU.00047.2011/ASSET/IMAGES/LARGE/ZH60061175900004.JPEG.
- Isales GM, Hipszer RA, Raftery TD, Chen A, Stapleton HM, Volz DC, 2015. Triphenyl phosphate-induced developmental toxicity in zebrafish: Potential role of the retinoic acid receptor. *Aquat. Toxicol.* 161, 221–230. 10.1016/j.aquatox.2015.02.009. [PubMed: 25725299]
- Kennard AS, Theriot JA, 2020. Osmolarity-independent electrical cues guide rapid response to injury in zebrafish epidermis. *eLife* 9, 1–27. 10.7554/ELIFE.62386.
- Kumai Y, Perry SF, 2012. Mechanisms and regulation of Na⁺ uptake by freshwater fish. *Respir. Physiol. Neurobiol.* 184 (3), 249–256. 10.1016/J.RESP.2012.06.009. [PubMed: 22698881]
- LeBert DC, Huttenlocher A, 2014. Inflammation and wound repair. *Semin. Immunol.* 26 (4), 315–320. 10.1016/j.smim.2014.04.007. [PubMed: 24853879]
- Manzon LA, 2002. The role of prolactin in fish osmoregulation: a review. *Gen. Comp. Endocrinol.* 125 (2), 291–310. 10.1006/GCEN.2001.7746. *Fish Osmoregulation: A Review. General and Comparative Endocrinology*, 125(2), 291–310. //10.1006/GCEN.2001.7746 [PubMed: 11884075]
- McCormick SD, Bradshaw D, 2006. Hormonal control of salt and water balance in vertebrates. *Gen. Comp. Endocrinol.* 147 (1), 3–8. 10.1016/J.YGCEN.2005.12.009. [PubMed: 16457828]
- McGee SP, Konstantinov A, Stapleton HM, Volz DC, 2013. Aryl phosphate esters within a major pentaBDE replacement product induce cardiotoxicity in developing zebrafish embryos: Potential role of the aryl hydrocarbon receptor. *Toxicol. Sci.* 133 (1), 144–156. 10.1093/toxsci/kft020. [PubMed: 23377616]
- Mitchell CA, Dasgupta S, Zhang S, Stapleton HM, Volz DC, 2018. Disruption of nuclear receptor signaling alters triphenyl phosphate-induced cardiotoxicity in zebrafish embryos. *Toxicol. Sci.* 163 (1), 307–318. 10.1093/toxsci/kfy037. [PubMed: 29529285]
- Mitchell CA, Reddam A, Dasgupta S, Zhang S, Stapleton HM, Volz DC, 2019. Diphenyl phosphate-induced toxicity during embryonic development. *Environ. Sci. Technol.* 53 (7), 3908–3916. 10.1021/acs.est.8b07238. [PubMed: 30864794]
- Papich MG, 2016. *Saunders Handbook of Veterinary Drugs*, 4th Edition. Elsevier Inc, Amsterdam.
- Peng G, He Y, Zhao M, Yu T, Qin Y, Lin S, 2018. Differential effects of metal oxide nanoparticles on zebrafish embryos and developing larvae. *Environ. Sci. Nano* 5 (5), 1200–1207. 10.1039/C8EN00190A.

- Reddam A, Mitchell CA, Dasgupta S, Kirkwood JS, Vollaro A, Hur M, Volz DC, 2019. mRNA-sequencing identifies liver as a potential target organ for triphenyl phosphate in embryonic zebrafish. *Toxicol. Sci.* 10.1093/toxsci/kfz169.
- Richardson RJ, 2018. Parallels between vertebrate cardiac and cutaneous wound healing and regeneration. *npj Regen. Med.* 3, 21. 10.1038/s41536-018-0059-y.
- Rombough P, 2007. The functional ontogeny of the teleost gill: Which comes first, gas or ion exchange? *Comp. Biochem. Physiol. A Mol. Integr. Physiol.* 148 (4), 732–742. 10.1016/j.cbpa.2007.03.007. [PubMed: 17451987]
- Rosowski EE, 2020. Determining macrophage versus neutrophil contributions to innate immunity using larval zebrafish. *DMM Dis. Models Mech.* 13 (1) 10.1242/DMM.041889/223112.
- Shu Y, Lou Q, Dai Z, Dai X, He J, Hu W, Yin Z, 2016. The basal function of teleost prolactin as a key regulator on ion uptake identified with zebrafish knockout models. *Sci. Rep.* 6 (1), 1–12. 10.1038/srep18597, 2016 6:1. [PubMed: 28442746]
- Szymalski Ł, Skopek R, Palusińska M, Schenk T, Stengel S, Lewicki S, Kraj L, Kamiński P, Zelent A, 2020. Retinoic acid and its derivatives in skin. *Cells* 9 (12), 1–14. 10.3390/cells9122660.
- Takada M, Kasai M, 2003. Prolactin increases open-channel density of epithelial Na⁺ channel in adult frog skin. *J. Exp. Biol.* 206 (Pt 8), 1319–1323. 10.1242/JEB.00266. [PubMed: 12624167]
- Wiegand J, Avila-Barnard S, Nemarugommula C, Lyons D, Zhang S, Stapleton HM, Volz DC, 2023. Triphenyl phosphate-induced pericardial edema in zebrafish embryos is dependent on the ionic strength of exposure media. *Environ. Int.* 173, 107757 10.1016/J.ENVINT.2023.107757.
- Wiegand J, Cheng V, Reddam A, Avila-Barnard S, Volz DC, 2022. Triphenyl phosphate-induced pericardial edema is associated with elevated epidermal ionocytes within zebrafish embryos. *Environ. Toxicol. Pharmacol.* 89, 103776 10.1016/j.etap.2021.103776. [PubMed: 34798236]
- Wright PA, Wood CM, 2012. Seven things fish know about ammonia and we don't. *Respir. Physiol. Neurobiol.* 184 (3), 231–240. 10.1016/J.RESP.2012.07.003. [PubMed: 22910326]
- Yozzo K, Isales G, Rafferty TD, Volz D, 2013. High-content screening assay for identification of chemicals impacting cardiovascular function in zebrafish embryos. *Environ. Sci. Technol.* 47 (19), 11302–11310. 10.1021/ES403360Y. [PubMed: 24015875]

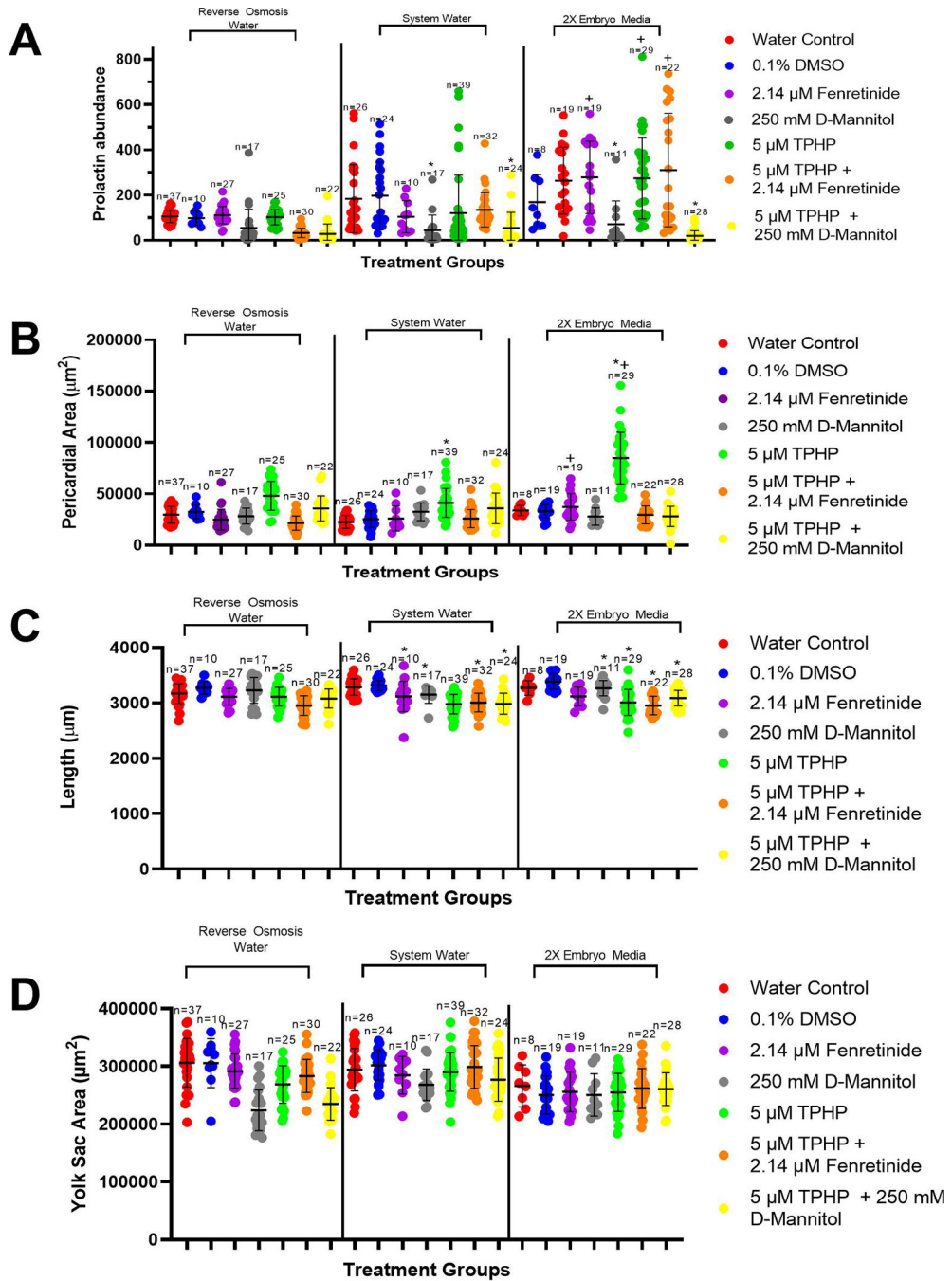


Fig. 1. Mean (\pm standard deviation) prolactin fluorescence area (A), pericardial area (B), body length (C), and yolk sac area (D) of embryos exposed to water only, vehicle (0.1 % DMSO), 2.14 µM Fenretinide, 250 mM D-Mannitol, 5 µM TPHP, 5 µM TPHP + 2.14 µM Fenretinide, or 5 µM TPHP + 250 mM D-Mannitol from 24–72 hpf. Plus sign (+) denotes a significant difference ($p < 0.05$) relative to the same treatment in RO water, whereas asterisk (*) denotes a significant difference ($p < 0.05$) relative to embryos exposed to vehicle (0.1 % DMSO) within the same media group (RO Water, System Water or 2X EM).

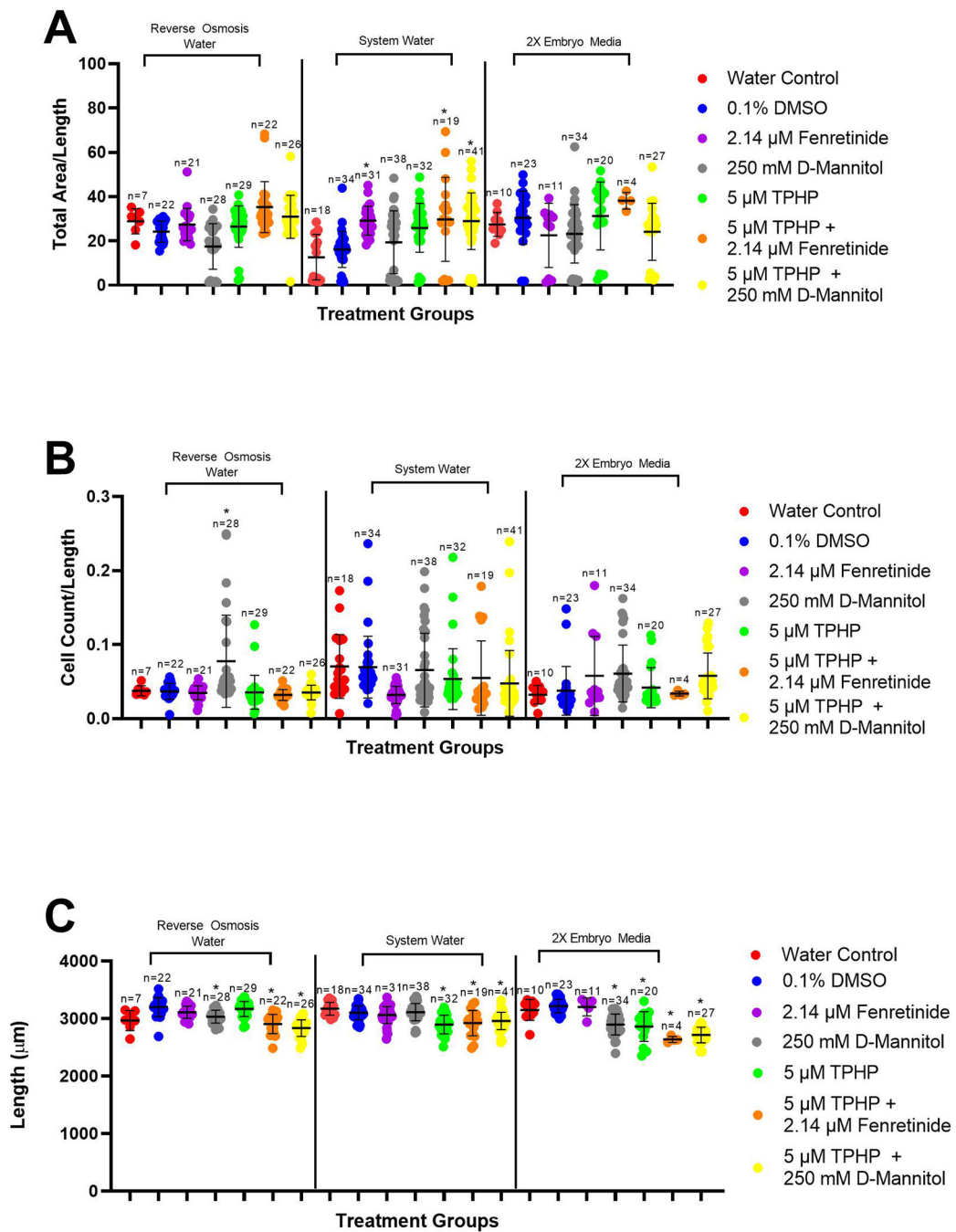


Fig. 2. Mean (\pm standard deviation) nuclei area (A) and cell count (B) normalized to the body length (C) of embryos exposed to water only, vehicle (0.1 % DMSO), 2.14 μM Fenretinide, 250 mM D-Mannitol, 5 μM TPHP, 5 μM TPHP + 2.14 μM Fenretinide, or 5 μM TPHP + 250 mM D-Mannitol from 24–72 hpf. Plus sign (+) denotes a significant difference ($p < 0.05$) relative to the same treatment in RO Water, whereas asterisk (*) denotes a significant difference ($p < 0.05$) relative to embryos exposed to vehicle (0.1 % DMSO) within the same exposure media (RO Water, System Water or 2X EM).

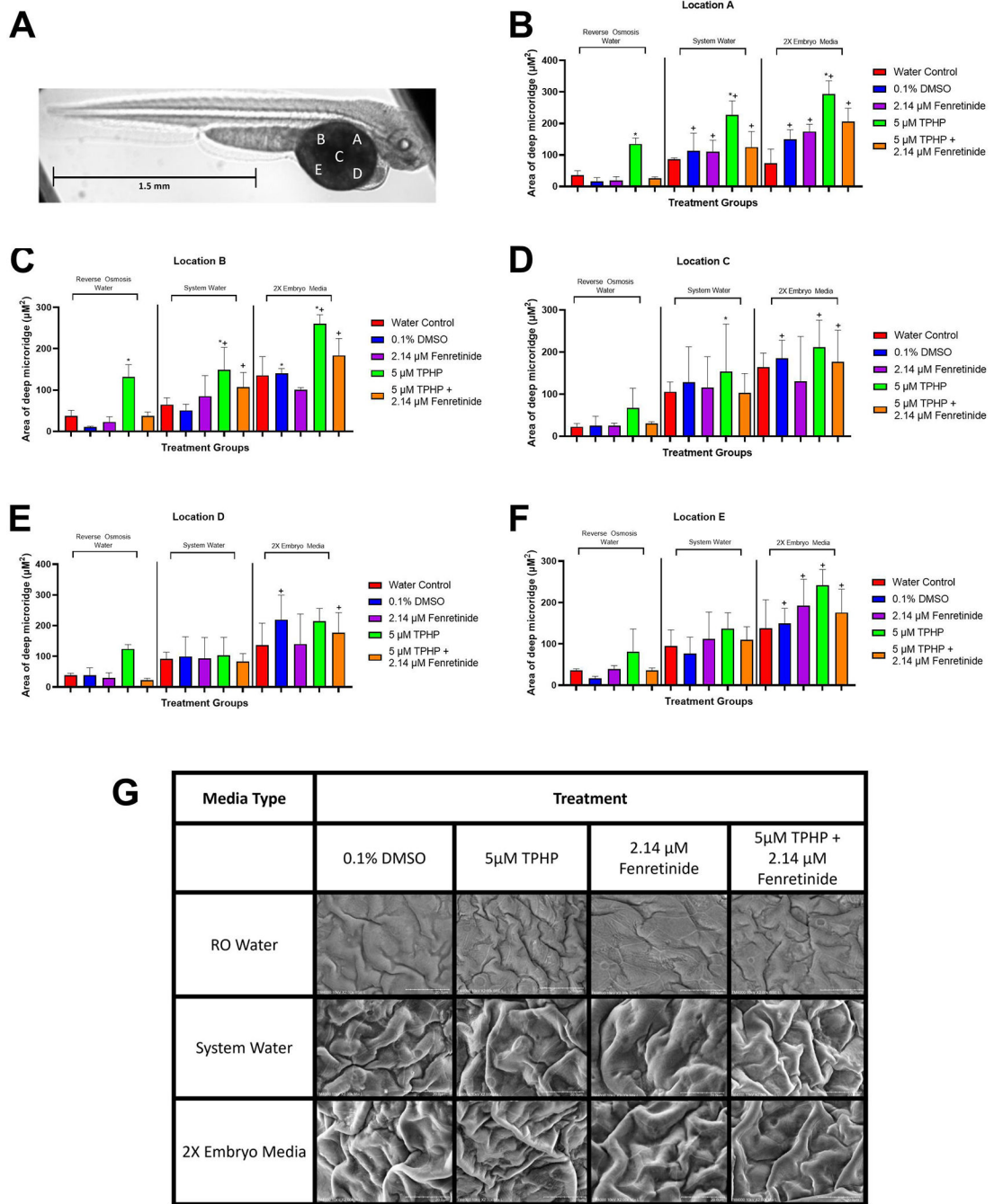


Fig. 3. Locations (A–E) used for SEM on the yolk sac epithelium of embryonic zebrafish (A). Panels B–F show the total area of epidermal folds across treatment groups within each location. Representative images of Location C are shown in Panel G. Asterisk (*) denotes a significant difference ($p < 0.05$) relative to vehicle (0.1 % DMSO) within same exposure medium. Plus sign (+) denotes a significant difference ($p < 0.05$) relative to 5 µM TPHP in Reverse Osmosis (RO) Water. Within Panel G, scale bars = 20 µm for all representative SEM images.

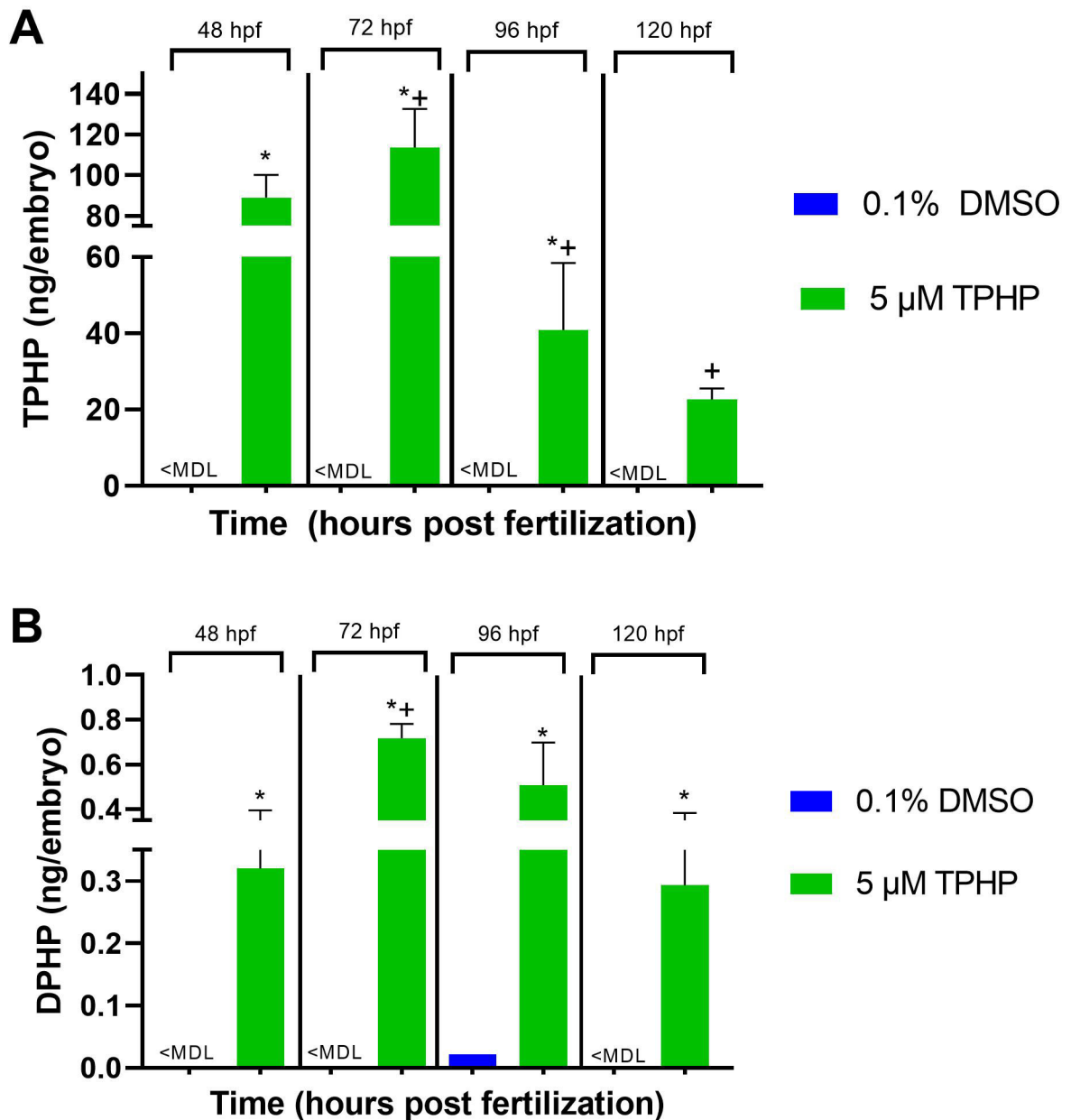


Fig. 4. Mean (\pm standard deviation) concentration of TPHP (ng/embryo) (A) and DPHP (ng/embryo) (B) in embryos exposed to vehicle (0.1 % DMSO) or 5 μ M TPHP from 24–72 hpf. Embryonic doses of TPHP and DPHP were quantified at 48 hpf, 72 hpf, 96 hpf, and 120 hpf. Asterisk (*) denotes a significant difference ($p < 0.05$) relative to vehicle (0.1 % DMSO) within the same time-point, whereas plus sign (+) denotes a significant difference ($p < 0.05$) relative to the same treatment at 48 hpf.

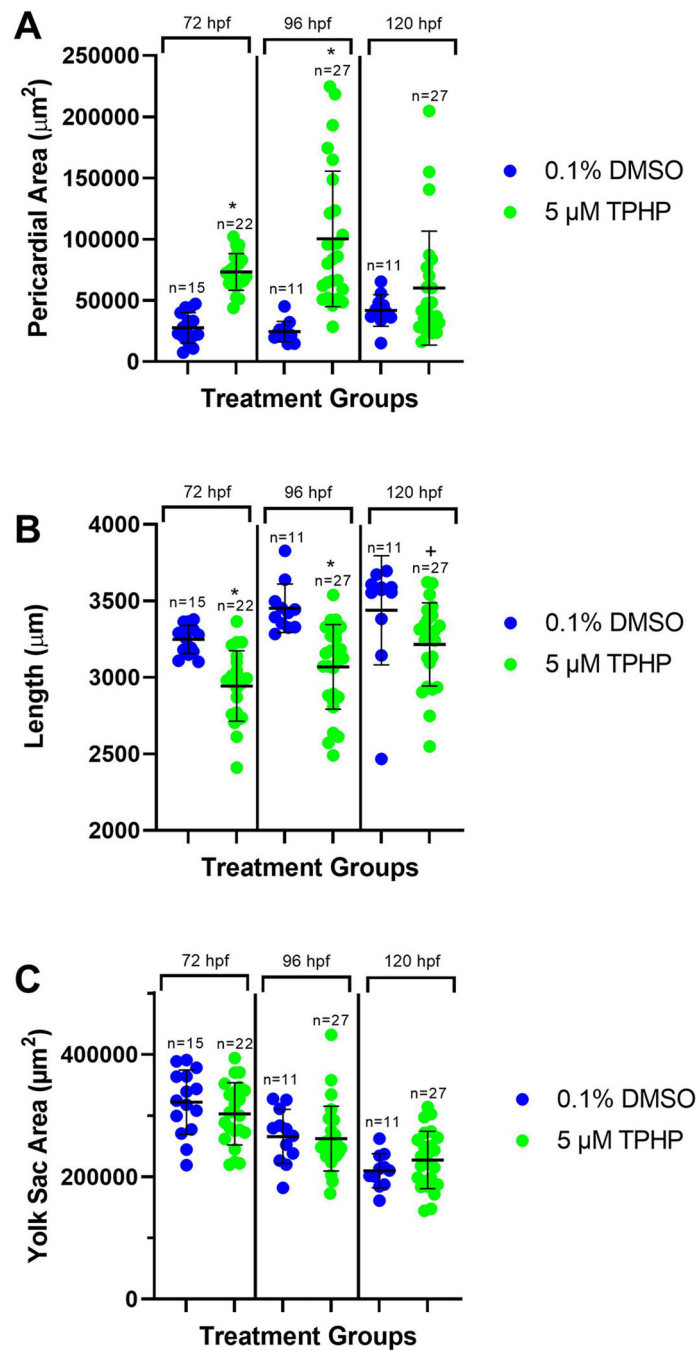


Fig. 5. Mean (\pm standard deviation) pericardial area (A), body length (B), and yolk sac area (C) of embryos exposed to vehicle (0.1 % DMSO) or 5 μM TPHP from 24–72 hpf and then clean System Water from 72–120 hpf. Asterisk (*) denotes a significant difference ($p < 0.05$) relative to vehicle (0.1 % DMSO) within the same time-point, whereas plus sign (+) denotes a significant difference ($p < 0.05$) relative to the same treatment at 48 hpf.